

Chapter 15

Stretch, fold, prune

I.1. Introduction to conjugacy problems for diffeomorphisms. This is a survey article on the area of global analysis defined by differentiable dynamical systems or equivalently the action (differentiable) of a Lie group G on a manifold M . Here $\text{Diff}(M)$ is the group of all diffeomorphisms of M and a diffeomorphism is a differentiable map with a differentiable inverse. (...) Our problem is to study the global structure, i.e., all of the orbits of M .

—Stephen Smale, *Differentiable Dynamical Systems*

WE HAVE LEARNED that the Rössler attractor is very thin, but otherwise the return maps that we found were disquieting – figure 3.3 did not appear to be a one-to-one map. This apparent loss of invertibility is an artifact of projection of higher-dimensional return maps onto their lower-dimensional subspaces. As the choice of a lower-dimensional subspace is arbitrary, the resulting snapshots of return maps look rather arbitrary, too. Such observations beg a question: Does there exist a natural, intrinsic coordinate system in which we should plot a return map?

We shall argue in sect. 15.1 that the answer is yes: The intrinsic coordinates are given by the stable/unstable manifolds, and a return map should be plotted as a map from the unstable manifold back onto the immediate neighborhood of the unstable manifold. In chapter 5 we established that Floquet multipliers of periodic orbits are (local) dynamical invariants. Here we shall show that every equilibrium point and every periodic orbit carries with it stable and unstable manifolds which provide topologically invariant *global* foliation of the state space. They will enable us to partition the state space in a dynamically invariant way, and assign symbolic dynamics itineraries to trajectories.

The topology of stretching and folding fixes the relative spatial ordering of trajectories, and separates the admissible and inadmissible itineraries. We illustrate how this works on Hénon map example 15.3. Determining which symbol sequences are absent, or ‘pruned’ is a formidable problem when viewed in the state

space, $[x_1, x_2, \dots, x_d]$ coordinates. It is equivalent to the problem of determining the location of all homoclinic tangencies, or all turning points of the Hénon attractor. They are dense on the attractor, and show no self-similar structure in the state space coordinates. However, in the ‘danish pastry’ representation of sect. 15.3 (and the ‘pruned danish,’ in American vernacular, of sect. 15.4), the pruning problem is visualized as crisply as the New York subway map; any itinerary which strays into the ‘pruned region’ is banned.

The level is distinctly cyclist, in distinction to the pedestrian tempo of the preceding chapter. Skip most of this chapter unless you really need to get into nitty-gritty details of symbolic dynamics.



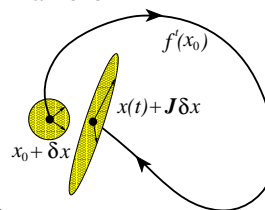
fast track:
chapter 16, p. 292

15.1 Goin’ global: stable/unstable manifolds

The complexity of this figure will be striking, and I shall not even try to draw it.

— H. Poincaré, on his discovery of homoclinic tangles, *Les méthodes nouvelles de la mécanique céleste*

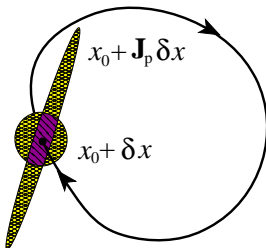
The Jacobian matrix J^t transports an infinitesimal neighborhood, its eigenvalues and eigen-directions describing deformation of an initial infinitesimal frame of



neighboring trajectories into a distorted frame time t later, as in figure 4.1.

Nearby trajectories separate exponentially along the unstable directions, approach each other along the stable directions, and creep along the marginal directions.

The fixed point q Jacobian matrix $J(x)$ eigenvectors (5.8) form a rectilinear coordinate frame in which the flow into, out of, or encircling the fixed point is



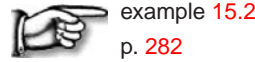
linear in the sense of sect. 4.3.

The continuations of the span of the local stable, unstable eigen-directions into global curvilinear invariant manifolds are called the *stable*, respectively *unstable manifolds*. They consist of all points which march into the fixed point forward,

respectively backward in time

$$\begin{aligned} W^s &= \{x \in \mathcal{M} : f^t(x) - x_q \rightarrow 0 \text{ as } t \rightarrow \infty\} \\ W^u &= \{x \in \mathcal{M} : f^{-t}(x) - x_q \rightarrow 0 \text{ as } t \rightarrow \infty\}. \end{aligned} \tag{15.1}$$

Eigenvectors $\mathbf{e}^{(i)}$ of the monodromy matrix $J(x)$ play a special role - on them the action of the dynamics is the linear multiplication by Λ_i (for a real eigenvector) along 1-dimensional invariant curve $W_{(i)}^{u,s}$ or spiral in/out action in a 2-D surface (for a complex pair). For $t \rightarrow \pm\infty$ a finite segment on $W_{(c)}^s$, respectively $W_{(e)}^u$ converges to the linearized map eigenvector $\mathbf{e}^{(c)}$, respectively $\mathbf{e}^{(e)}$, where $^{(c)}$, $^{(e)}$ stand respectively for ‘contracting,’ ‘expanding.’ In this sense each eigenvector defines a (curvilinear) axis of the stable, respectively unstable manifold.



example 15.2
p. 282

Actual construction of these manifolds is the converse of their definition (15.1): one starts with an arbitrarily small segment of a fixed point eigenvector and lets evolution stretch it into a finite segment of the associated manifold. As a periodic point x on cycle p is a fixed point of $f^{T_p}(x)$, the fixed point discussion that follows applies equally well to equilibria and periodic orbits.

Expanding real and positive Floquet multiplier. Consider i th expanding eigenvalue, eigenvector pair $(\Lambda_i, \mathbf{e}^{(i)})$ computed from $J = J_p(x)$ evaluated at a fixed point x ,

$$J(x)\mathbf{e}^{(i)}(x) = \Lambda_i\mathbf{e}^{(i)}(x), \quad x \in \mathcal{M}_p, \quad \Lambda_i > 1. \tag{15.2}$$

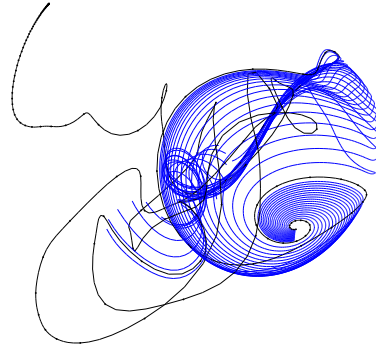
Take an infinitesimal eigenvector $\mathbf{e}^{(i)}(x)$, $\|\mathbf{e}^{(i)}(x)\| = \varepsilon \ll 1$, and its return $\Lambda_i\mathbf{e}^{(i)}(x)$ after one period T_p . Sprinkle the straight interval between $[\varepsilon, \Lambda_i\varepsilon] \subset W_{(i)}^u$ with a large number of points $x^{(k)}$, for example equidistantly spaced on logarithmic scale between $\ln \varepsilon$ and $\ln \Lambda_i + \ln \varepsilon$. The successive returns of these points $f^{T_p}(x^{(k)})$, $f^{2T_p}(x^{(k)})$, \dots , $f^{mT_p}(x^{(k)})$ trace out the 1d curve $W_{(i)}^u$ within the unstable manifold. As separations between points tend to grow exponentially, every so often one needs to interpolate new starting points between the rarified ones. Repeat for $-\mathbf{e}^{(i)}(x)$.

Contracting real and positive Floquet multiplier. Reverse the action of the map backwards in time. This turns a contracting direction into an expanding one, tracing out the curvilinear stable manifold $W_{(i)}^s$ as a continuation of $\mathbf{e}^{(i)}$.

Expanding/contracting real negative Floquet multiplier. As above, but every even iterate $f^{2T_p}(x^{(k)})$, $f^{4T_p}(x^{(k)})$, $f^{6T_p}(x^{(k)})$ continues in the direction $\mathbf{e}^{(i)}$, every odd one in the direction $-\mathbf{e}^{(i)}$.

Complex Floquet multiplier pair, expanding/contracting. The complex Floquet multiplier pair $\{\Lambda_j, \Lambda_{j+1} = \Lambda_j^*\}$ has Floquet exponents (4.8) of form $\lambda^{(j)} =$

Figure 15.1: A $2d$ unstable manifold obtained by continuation from the linearized neighborhood of a complex eigenvalue pair of an unstable equilibrium of plane Couette flow, a projection from a 61,506-dimensional state space ODE truncation of the (∞ -dimensional) Navier-Stokes PDE. (J.F. Gibson, 8 Nov. 2005 blog entry [5])

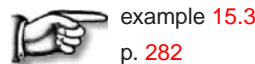


$\mu^{(j)} \pm i\omega^{(j)}$, with the sign of $\mu^{(k)} \neq 0$ determining whether the linear neighborhood is out / in spiralling. The orthogonal pair of real eigenvectors $\{\text{Re } \mathbf{e}^{(j)}, \text{Im } \mathbf{e}^{(j)}\}$ spans a plane. $T = 2\pi/\omega^{(j)}$ is the time of one turn of the spiral, $\mathcal{J}^T \text{Re } \mathbf{e}^{(j)}(x) = |\Lambda_j| \text{Re } \mathbf{e}^{(j)}(x)$. As in the real cases above, sprinkle the straight interval between $[\varepsilon, |\Lambda_j|\varepsilon]$ along $\text{Re } \mathbf{e}^{(j)}(x)$ with a large number of points $x^{(k)}$. The flow will now trace out the $2d$ invariant manifold as an out / in spiralling strip. Two low-dimensional examples are the unstable manifolds of the Lorenz flow, figure 14.8 (a), and the Rössler flow, figure 14.7 (a). For a highly non-trivial example, see figure 15.1.

The unstable manifolds of a flow are d_u -dimensional. Taken together with the marginally stable direction along the flow, they are rather hard to visualize. A more insightful visualization is offered by $(d-1)$ -dimensional Poincaré sections (3.2) with the marginal flow direction eliminated (see also sect. 3.1.2). Stable, unstable manifolds for maps are defined by

$$\begin{aligned} \hat{W}^s &= \{x \in \mathcal{P} : P^n(x) - x_q \rightarrow 0 \text{ as } n \rightarrow \infty\} \\ \hat{W}^u &= \{x \in \mathcal{P} : P^{-n}(x) - x_q \rightarrow 0 \text{ as } n \rightarrow \infty\}, \end{aligned} \tag{15.3}$$

where $P(x)$ is the $(d-1)$ -dimensional return map (3.1). In what follows, all invariant manifolds W^u, W^s will be restricted to their Poincaré sections \hat{W}^u, \hat{W}^s .



example 15.3
p. 282

In general the full state space eigenvectors do not lie in a Poincaré section; the eigenvectors $\hat{\mathbf{e}}^{(j)}$ tangent to the section are given by (5.20). Furthermore, while in the linear neighborhood of fixed point x the trajectories return with approximate periodicity T_p , this is not the case for the globally continued manifolds; $\tau(x)$, or the first return times (3.1) differ, and the $\hat{W}_{(j)}^u$ restricted to the Poincaré section is obtained by continuing trajectories of the points from the full state space curve $W_{(j)}^u$ to the section \mathcal{P} .

For long times the unstable manifolds wander throughout the connected ergodic component, and are no more informative than an ergodic trajectory. For example, the line with equitemporal knots in figure 15.1 starts out on a smoothly

curved neighborhood of the equilibrium, but after a ‘turbulent’ episode decays into an attractive equilibrium point. The trick is to stop continuing an invariant manifold while the going is still good.

15.2 Horseshoes

If you find yourself mystified by Smale's article abstract quoted on page 266, about 'the action (differentiable) of a Lie group G on a manifold M ,' time has come to bring Smale to everyman. If you still remain mystified by the end of this chapter, reading chapter 19 might help; for example, the Liouville operators form a Lie group of symplectic, or canonical transformations acting on the (p, q) manifold.

If a flow is locally unstable but globally bounded, any open ball of initial points will be stretched out and then folded. An example is a 3-dimensional invertible flow sketched in figure 14.7 (a) which returns a Poincaré section of the flow folded into a 'horseshoe' (we shall belabor this in figure 15.4). We now offer two examples of locally unstable but globally bounded flows which return an initial area stretched and folded into a 'horseshoe,' such that the initial area

exercise 15.1

Figure 15.2: Binary labeling of trajectories of the symmetric 3-disk pinball; a bounce in which the trajectory returns to the preceding disk is labeled 0, and a bounce which results in continuation to the third disk is labeled 1.

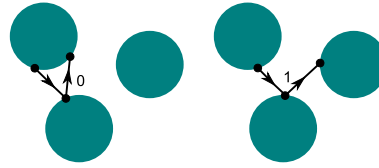
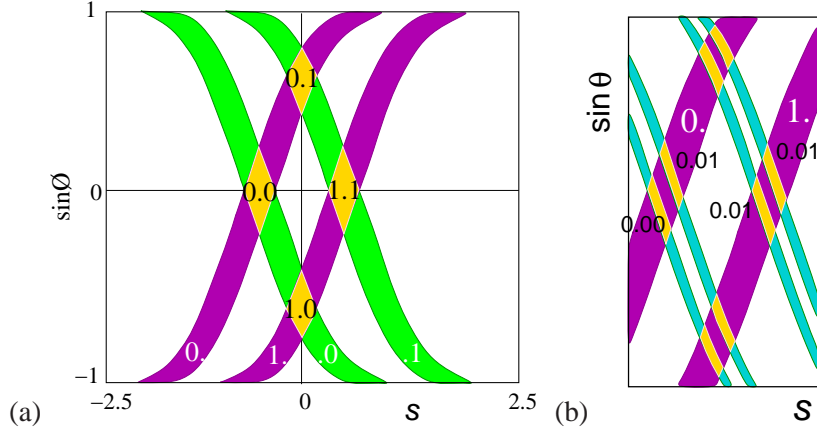



Figure 15.3: The 3-disk game of pinball of figure 14.5, generated by starting from disk 1, preceded by disk 2, coded in binary, as in figure 15.2. (a) Strips $\mathcal{M}_{s_i,j}$ which have survived a bounce in the past and will survive a bounce in the future. (b) Iteration corresponds to the decimal point shift; for example, all points in the rectangle [1.01] map into the rectangles [0.10], [0.11] in one iteration.




is intersected at most twice. We shall refer to such mappings with at most 2^n transverse self-intersections at the n th iteration as the *once-folding* maps.

The first example is the 3-disk game of pinball figure 14.5, which, for sufficiently separated disks (see figure 14.6), is an example of a complete Smale horseshoe. We start by exploiting its symmetry to simplify it, and then partition its state space by its stable / unstable manifolds.



 example 15.4
p. 283

The 3-disk repeller does not really look like a ‘horseshoe;’ the ‘fold’ is cut out of the picture by allowing the pinballs that fly between the disks to fall off the table and escape. Next example captures the ‘stretch & fold’ horseshoe dynamics of return maps such as Rössler’s, figure 3.2.

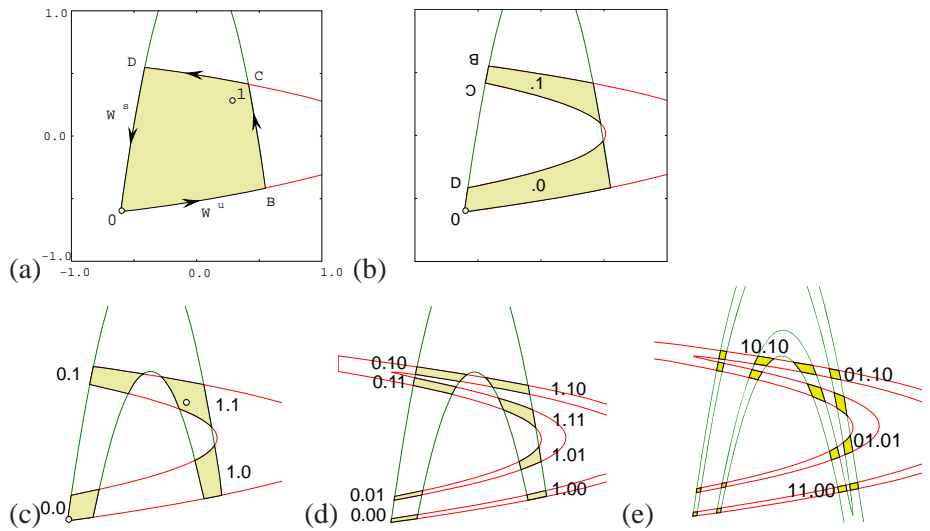
 example 15.5
p. 283

What is the significance of the subscript such as $_{.011}$ which labels the \mathcal{M}_{011} future strip? The two strips $\mathcal{M}_0, \mathcal{M}_1$ partition the state space into two regions labeled by the two-letter alphabet $\mathcal{A} = \{0, 1\}$. $S^+ = .011$ is the *future itinerary* for all $x \in \mathcal{M}_{011}$. Likewise, for the past strips all $x \in \mathcal{M}_{s_{-m} \dots s_{-1} s_0}$ have the *past itinerary* $S^- = s_{-m} \dots s_{-1} s_0$. Which partition we use to present pictorially the regions that do not escape in m iterations is a matter of taste, as the backward strips are the preimages of the forward ones

$$\mathcal{M}_0 = f(\mathcal{M}_0), \quad \mathcal{M}_1 = f(\mathcal{M}_1).$$

Ω , the non-wandering set (2.3) of \mathcal{M} , is the union of all points whose forward

Figure 15.4: The Hénon map (15.20) for $a = 6$, $b = -1$: fixed point $\bar{0}$ with segments of its stable, unstable manifolds W^s , W^u , and fixed point $\bar{1}$. (a) Their intersection bounds the region $\mathcal{M} = 0BCD$ which contains the non-wandering set Ω . (b) The intersection of the forward image $f(\mathcal{M})$ with \mathcal{M} consists of two (future) strips $\mathcal{M}_0, \mathcal{M}_{1,2}$ with points BCD brought closer to fixed point $\bar{0}$ by the stable manifold contraction. (c) The intersection of the forward image $f(\mathcal{M})$ with the backward backward $f^{-1}(\mathcal{M})$ is a four-region cover of Ω . (d) The intersection of the twice-folded forward horseshoe $f^2(\mathcal{M})$ with backward horseshoe $f^{-2}(\mathcal{M})$. (e) The intersection of $f^2(\mathcal{M})$ with $f^{-2}(\mathcal{M})$. Iteration yields the complete Smale horseshoe non-wandering set Ω , i.e., the union of all non-wandering points of f , with every forward fold intersecting every backward fold. (P. Cvitanović and Y. Matsuoka)



and backward trajectories remain trapped for all time, given by the intersections of all images and preimages of \mathcal{M} :

$$\Omega = \left\{ x \mid x \in \lim_{m,n \rightarrow \infty} f^m(\mathcal{M}) \cap f^{-n}(\mathcal{M}) \right\}. \tag{15.6}$$

Two important properties of the Smale horseshoe are that it has a *complete binary symbolic dynamics* and that it is *structurally stable*.

For a *complete* Smale horseshoe every forward fold $f^n(\mathcal{M})$ intersects transversally every backward fold $f^{-m}(\mathcal{M})$, so a unique bi-infinite binary sequence can be associated to every element of the non-wandering set. A point $x \in \Omega$ is labeled by the intersection of its past and future itineraries $S(x) = \cdots s_{-2}s_{-1}s_0.s_1s_2\cdots$, where $s_n = s$ if $f^n(x) \in \mathcal{M}_s$, $s \in \{0, 1\}$ and $n \in \mathbb{Z}$.

remark A.1

The system is said to be *structurally stable* if all intersections of forward and backward iterates of \mathcal{M} remain transverse for sufficiently small perturbations $f \rightarrow f + \delta$ of the flow, for example, for slight displacements of the disks in the pinball problem, or sufficiently small variations of the Hénon map parameters a, b . While structural stability is exceedingly desirable, it is also exceedingly rare. About this,

section 1.8

section 24.2

15.3 Symbol plane

Consider a system for which you have succeeded in constructing a covering symbolic dynamics, such as a well-separated 3-disk system. Now start moving the disks toward each other. At some critical separation a disk will start blocking families of trajectories traversing the other two disks. The order in which trajectories disappear is determined by their relative ordering in space; the ones closest

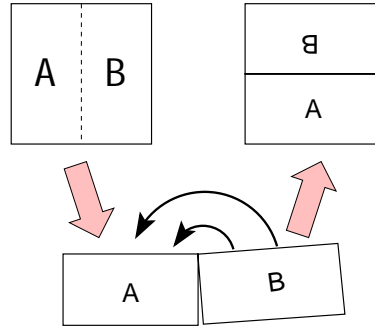


Figure 15.5: Kneading orientation preserving danish pastry: mimic the horseshoe dynamics of figure 15.6 by: (1) squash the unit square by factor 1/2, (2) stretch it by factor 2, and (3) fold the right half back over the left half.

to the intervening disk will be pruned first. Determining inadmissible itineraries requires that we relate the spatial ordering of trajectories to their time ordered itineraries.

exercise 15.8

So far we have rules that, given a state space partition, generate a *temporally* ordered itinerary for a given trajectory. Our next task is the converse: given a set of itineraries, what is the *spatial* ordering of corresponding points along the trajectories? In answering this question we will be aided by Smale’s visualization of the relation between the topology of a flow and its symbolic dynamics by means of ‘horseshoes,’ such as figure 15.4.

15.3.1 Kneading danish pastry

The danish pastry transformation, the simplest baker’s transformation appropriate to Hénon type mappings, yields a binary coordinatization of all possible periodic points.

The symbolic dynamics of once-folding map is given by the danish pastry transformation. This generates both the longitudinal and transverse alternating binary tree. The longitudinal coordinate is given by the head of a symbolic sequence; the transverse coordinate is given by the tail of the symbolic sequence. The dynamics on this space is given by symbol shift permutations; volume preserving, with 2 expansion and 1/2 contraction.

For a better visualization of 2-dimensional non-wandering sets, fatten the intersection regions until they completely cover a unit square, as in figure 15.7. We shall refer to such a ‘map’ of the topology of a given ‘stretch & fold’ dynamical system as the *symbol square*. The symbol square is a topologically accurate representation of the non-wandering set and serves as a street map for labeling its pieces. Finite memory of m steps and finite foresight of n steps partitions the symbol square into *rectangles* $[s_{-m+1} \cdots s_0.s_1s_2 \cdots s_n]$, such as those of figure 15.6. In the binary dynamics symbol square the size of such rectangle is $2^{-m} \times 2^{-n}$; it corresponds to a region of the dynamical state space which contains all points that share common n future and m past symbols. This region maps in a nontrivial way in the state space, but in the symbol square its dynamics is exceedingly simple; all of its points are mapped by the decimal point shift (14.13)

exercise 15.3
exercise 15.4

$$\sigma(\cdots s_{-2}s_{-1}s_0.s_1s_2s_3 \cdots) = \cdots s_{-2}s_{-1}s_0.s_1s_2s_3 \cdots, \tag{15.7}$$

Figure 15.6: The dynamics maps two (past) strips M_0, M_1 into two (future) strips M_0, M_1 . The corners are labeled to aid visualization. Note that the $BCGH$ strip is rotated by 180 degrees. (P. Cvitanović and Y. Matsuoka)

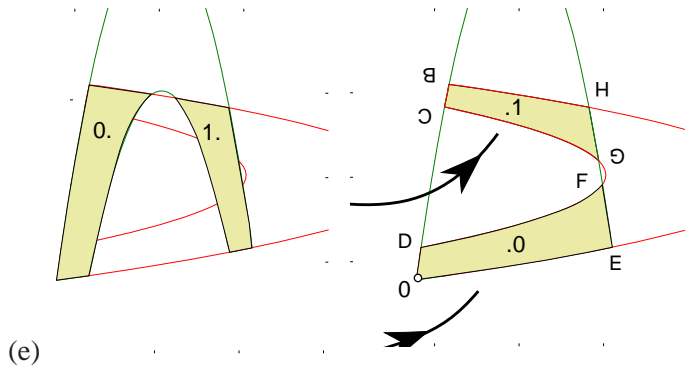
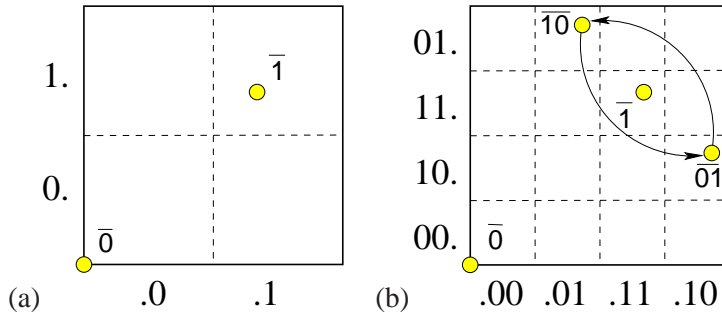


Figure 15.7: Kneading danish pastry: symbol square representation of an orientation preserving once-folding map obtained by fattening the Smale horseshoe intersections of (a) figure 15.6 (b) figure 15.4 into a unit square. Also indicated: the fixed points $\bar{0}, \bar{1}$ and the 2-cycle points $\{0\bar{1}, \bar{1}0\}$. In the symbol square the dynamics maps rectangles into rectangles by a decimal point shift.



Example 15.1 A Hénon repeller subshift: (continued from example 15.5) The Hénon map acts on the binary partition as a shift map. Figure 15.6 illustrates action $f(M_0) = M_0$. The square $[01.01]$ gets mapped into the rectangles $\sigma[01.01] = [10.1] = \{[10.10], [10.11]\}$, see figure 15.4 (e). Further examples can be gleaned from figure 15.4.

As the horseshoe mapping is a simple repetitive operation, we expect a simple relation between the symbolic dynamics labeling of the horseshoe strips, and their relative placement. The symbol square points $\gamma(S^+)$ with future itinerary S^+ are constructed by converting the sequence of s_n 's into a binary number by the algorithm (14.4). This follows by inspection from figure 15.9. In order to understand this relation between the topology of horseshoes and their symbolic dynamics, it might be helpful to backtrace to sect. 14.4 and work through and understand first the symbolic dynamics of 1-dimensional unimodal mappings.

Under backward iteration the roles of 0 and 1 symbols are interchanged; M_0^{-1} has the same orientation as M , while M_1^{-1} has the opposite orientation. We assign to an orientation preserving once-folding map the past topological coordinate $\delta = \delta(S^-)$ by the algorithm:

exercise 15.5

$$w_{n-1} = \begin{cases} w_n & \text{if } s_n = 0 \\ 1 - w_n & \text{if } s_n = 1 \end{cases}, \quad w_0 = s_0$$

$$\delta(S^-) = 0.w_0w_{-1}w_{-2}\dots = \sum_{n=1}^{\infty} w_{1-n}/2^n. \quad (15.8)$$

Such formulas are best derived by solitary contemplation of the action of a folding map, in the same way we derived the future topological coordinate (14.4).

Figure 15.8: Kneading orientation preserving danish pastry: symbol square representation of an orientation preserving once-folding map obtained by fattening the intersections of two forward iterates / two backward iterates of Smale horseshoe into a unit square.

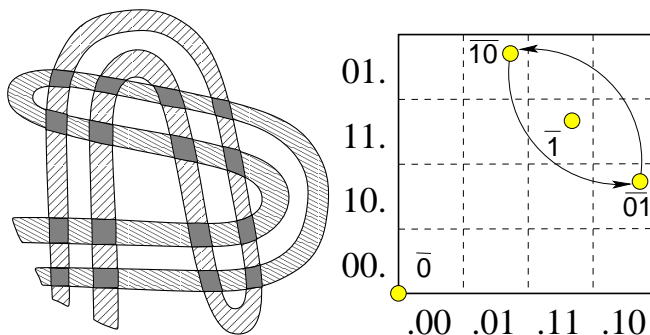
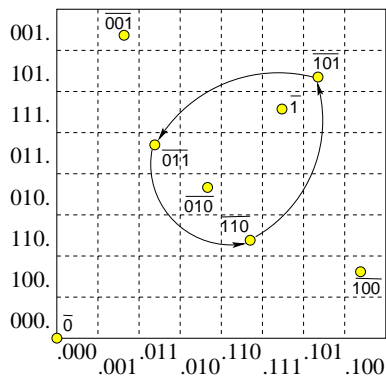


Figure 15.9: Kneading danish pastry: symbol square representation of an orientation preserving once-folding map obtained by fattening the Smale horseshoe intersections of figure 15.4 (e) into a unit square. Also indicated: the fixed points $\bar{0}$, $\bar{1}$, and the 3-cycle points $\{011, 110, 101\}$. In the symbol square the dynamics maps rectangles into rectangles by a decimal point shift.



The coordinate pair (δ, γ) associates a point (x, y) in the state space Cantor set of figure 15.4 to a point in the symbol square of figure 15.9, preserving the topological ordering. The symbol square $[\delta, \gamma]$ serves as a topologically faithful representation of the non-wandering set of any once-folding map, and aids us in partitioning the set and ordering the partitions for any flow of this type.

Résumé

In the preceding and this chapter we start with a d -dimensional state space and end with a 1-dimensional return map description of the dynamics. The arc-length parametrization of the unstable manifold maintains the 1-to-1 relation of the *full* d -dimensional state space dynamics and its 1-dimensional return-map representation. To high accuracy *no information about the flow is lost* by its 1-dimensional return map description. We explain why Lorenz equilibria are heteroclinically connected (it is not due to the symmetry), and how to generate all periodic orbits of Lorenz flow up to given length. This we do, in contrast to the rest of the thesis, without any group-theoretical jargon to blind you with.

For 1-dimensional maps the folding point is the critical point, and easy to determine. In higher dimensions, the situation is not so clear - one can attempt to determine the (fractal set of) folding points by looking at their higher iterates - due to the contraction along stable manifolds, the fold gets to be exponentially sharper at each iterate. In practice this set is essentially uncontrollable for the same reason the flow itself is chaotic - exponential growth of errors. We prefer to determine a folding point by bracketing it by longer and longer cycles which can

be determined accurately using variational methods of chapter 33, irrespective of their period.

For a generic dynamical system a subshift of finite type is the exception rather than the rule. Its symbolic dynamics can be arbitrarily complex; even for the logistic map the grammar is finite only for special parameter values. Only some repelling sets (like our game of pinball) and a few purely mathematical constructs (called Anosov flows) are structurally stable - for most systems of interest an infinitesimal perturbation of the flow destroys and/or creates an infinity of trajectories, and specification of the grammar requires determination of pruning blocks of arbitrary length. The repercussions are dramatic and counterintuitive; for example, the transport coefficients such as the deterministic diffusion constant of sect. 24.2 are emphatically *not* smooth functions of the system parameters. The importance of symbolic dynamics is often under appreciated; as we shall see in chapters 23 and 28, the existence of a finite grammar is the crucial prerequisite for construction of zeta functions with nice analyticity properties. This generic lack of structural stability is what makes nonlinear dynamics so hard.

The conceptually simpler finite subshift Smale horseshoes suffice to motivate most of the key concepts that we shall need for time being. Our strategy is akin to bounding a real number by a sequence of rational approximants; we converge toward the non-wandering set under investigation by a sequence of self-similar Cantor sets. The rule that everything to one side of the pruning front is forbidden is striking in its simplicity: instead of pruning a Cantor set embedded within some larger Cantor set, the pruning front cleanly cuts out a *compact* region in the symbol square, and that is all - there are no additional pruning rules. A ‘self-similar’ Cantor set (in the sense in which we use the word here) is a Cantor set equipped with a *subshift of finite type* symbol dynamics, i.e., the corresponding grammar can be stated as a finite number of pruning rules, each forbidding a finite subsequence $_s_1 s_2 \dots s_n _$. Here the notation $_s_1 s_2 \dots s_n _$ stands for n consecutive symbols s_1, s_2, \dots, s_n , preceded and followed by arbitrary symbol strings.

The symbol square is a useful tool in transforming topological pruning into pruning rules for inadmissible sequences; those are implemented by constructing transition matrices and/or graphs, see chapters 17 and 18.

Example 15.5 A Hénon repeller complete horseshoe: (continued from example 3.6) Consider 2-dimensional Hénon map

exercise 3.5

$$(x_{n+1}, y_{n+1}) = (1 - ax_n^2 + by_n, x_n). \quad (15.20)$$

If you start with a small ball of initial points centered around the fixed point x_0 , and iterate the map, the ball will be stretched and squashed along the unstable manifold W_0^u . Iterated backward in time,

$$(x_{n-1}, y_{n-1}) = (y_n, -b^{-1}(1 - ay_n^2 - x_n)), \quad (15.21)$$

this small ball of initial points traces out the stable manifold W_0^s . Their intersections enclose the region \mathcal{M} , figure 15.4(a). Any point outside W_0^s border of \mathcal{M} escapes to infinity forward in time, while –by time reversal– any point outside W_0^u border arrives from infinity back in paste. In this way the unstable - stable manifolds define topologically, invariant and optimal initial region \mathcal{M} ; all orbits that stay confined for all times are confined to \mathcal{M} .

The Hénon map models qualitatively the Poincaré section return map of figure 14.7(b). For $b = 0$ the Hénon map reduces to the parabola (14.5), and, as shown in sects. 3.3 and 33.1, for $b \neq 0$ it is kind of a fattened parabola; by construction, it takes a rectangular initial area and returns it bent as a horseshoe. Parameter a controls the amount of stretching, while the parameter b controls the amount of compression of the folded horseshoe. For definitiveness, fix the parameter values to $a = 6$, $b = -1$; the map is then strongly stretching but area preserving, the furthest away from the strongly dissipative examples discussed in sect. 14.2. The map is quadratic, so it has 2 fixed points $x_0 = f(x_0)$, $x_1 = f(x_1)$ indicated in figure 15.4(a). For the parameter values at hand, they are both unstable.

Iterated one step forward, the region \mathcal{M} is stretched and folded into a Smale horseshoe drawn in figure 15.4(b). Label the two forward intersections $f(\mathcal{M}) \cap \mathcal{M}$ by \mathcal{M}_s , with $s \in \{0, 1\}$. The horseshoe consists of the two strips $\mathcal{M}_0, \mathcal{M}_1$, and the bent segment that lies entirely outside the W_0^s line. As all points in this segment escape to infinity under forward iteration, this region can safely be cut out and thrown away.

Iterated one step backwards, the region \mathcal{M} is again stretched and folded into a horseshoe, figure 15.4(c). As stability and instability are interchanged under time reversal, this horseshoe is transverse to the forward one. Again the points in the horseshoe bend wander off to infinity as $n \rightarrow -\infty$, and we are left with the two (past) strips $\mathcal{M}_0, \mathcal{M}_1$. Iterating two steps forward we obtain the four strips $\mathcal{M}_{11}, \mathcal{M}_{01}, \mathcal{M}_{00}, \mathcal{M}_{10}$, and iterating backwards we obtain the four strips $\mathcal{M}_{00}, \mathcal{M}_{01}, \mathcal{M}_{11}, \mathcal{M}_{10}$ transverse to the forward ones just as for 3-disk pinball game figure 15.2. Iterating three steps forward we get an 8 strips, and so on ad infinitum. (continued in example 15.1)

[click to return: p. 267](#)

Exercises

15.1. **A Smale horseshoe.** The Hénon map of example 3.6

$$\begin{bmatrix} x' \\ y' \end{bmatrix} = \begin{bmatrix} 1 - ax^2 + by \\ x \end{bmatrix} \quad (15.25)$$

maps the $[x, y]$ plane into itself - it was constructed by Hénon [6] in order to mimic the Poincaré section of once-folding map induced by a flow like the one sketched in figure 14.7. For definitiveness fix the parameters to $a = 6, b = -1$.

- Draw a rectangle in the (x, y) plane such that its n th iterate by the Hénon map intersects the rectangle 2^n times.
- Construct the inverse of the (15.25).
- Iterate the rectangle back in the time; how many intersections are there between the n forward and m backward iterates of the rectangle?
- Use the above information about the intersections to guess the (x, y) coordinates for the two fixed points, a 2-periodic point, and points on the two distinct 3-cycles from table 18.1. The exact periodic points are computed in exercise 16.11.

15.2. **A simple stable/unstable manifolds pair.** Integrate flow (15.12), verify (15.13). Check that the projection matrices \mathbf{P}_i (15.16) are orthonormal and complete. Use them to construct right and left eigenvectors; check that they are mutually orthogonal. Explain why is (15.17) the equation for the stable manifold. (N. Lebovitz)

15.3. **Kneading Danish pastry.** Write down the $(x, y) \rightarrow (x, y)$ mapping that implements the baker's map

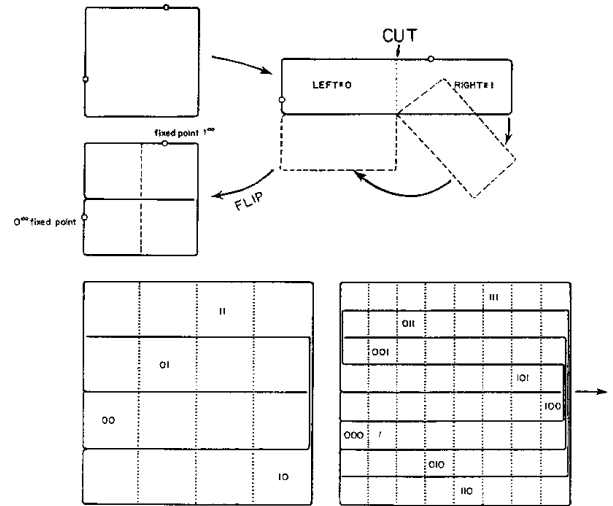


FIG. 4. Iterative construction of the symbol plane.

Figure: *Kneading danish pastry: symbol square representation of an orientation reversing once-folding map obtained by fattening the Smale horseshoe intersections of figure 15.4 into a unit square. In the symbol square the dynamics maps rectangles into rectangles by a decimal point shift. together with the inverse mapping.*

Sketch a few rectangles in symbol square and their forward and backward images. (Hint: the mapping is very much like the tent map (14.20)).

15.4. **Kneading danish without flipping.** The baker's map of exercise 15.3 includes a flip - a map of this type is called an orientation reversing once-folding map. Write down the $(x, y) \rightarrow (x, y)$ mapping that implements an orientation preserving baker's map (no flip; Jacobian determinant = 1). Sketch and label the first few folds of the symbol square.

15.5. **Orientation reversing once-folding map.** By adding a reflection around the vertical axis to the horseshoe map g we get the orientation reversing map \tilde{g} shown in the second Figure above. \tilde{Q}_0 and \tilde{Q}_1 are oriented as Q_0 and Q_1 , so the definition of the future topological coordinate γ is identical to the γ for the orientation preserving horseshoe. The inverse intersections \tilde{Q}_0^{-1} and \tilde{Q}_1^{-1} are oriented so that \tilde{Q}_0^{-1} is opposite to Q_0 , while \tilde{Q}_1^{-1} has the same orientation as Q_0 . Check that the past topological

coordinate δ is given by

$$w_{n-1} = \begin{cases} 1 - w_n & \text{if } s_n = 0 \\ w_n & \text{if } s_n = 1 \end{cases}, \quad w_0 = s_0$$

$$\delta(x) = 0.w_0w_{-1}w_{-2}\dots = \sum_{n=1}^{\infty} w_{1-n}/2^n \quad (15.26)$$

15.6. Infinite symbolic dynamics. Let σ be a function that returns zero or one for every infinite binary string: $\sigma : \{0, 1\}^{\mathbb{N}} \rightarrow \{0, 1\}$. Its value is represented by $\sigma(\epsilon_1, \epsilon_2, \dots)$ where the ϵ_i are either 0 or 1. We will now define an operator \mathcal{T} that acts on observables on the space of binary strings. A function a is an observable if it has bounded variation, that is, if

$$\|a\| = \sup_{\{\epsilon_i\}} |a(\epsilon_1, \epsilon_2, \dots)| < \infty.$$

For these functions

$$\mathcal{T}a(\epsilon_1, \epsilon_2, \dots) = a(0, \epsilon_1, \epsilon_2, \dots)\sigma(0, \epsilon_1, \epsilon_2, \dots) + a(1, \epsilon_1, \epsilon_2, \dots)\sigma(1, \epsilon_1, \epsilon_2, \dots).$$

(a) (easy) Consider a finite version T_n of the operator \mathcal{T} :

$$T_n a(\epsilon_1, \epsilon_2, \dots, \epsilon_{1,n}) = a(0, \epsilon_1, \epsilon_2, \dots, \epsilon_{n-1})\sigma(0, \epsilon_1, \epsilon_2, \dots, \epsilon_{n-1}) + a(1, \epsilon_1, \epsilon_2, \dots, \epsilon_{n-1})\sigma(1, \epsilon_1, \epsilon_2, \dots, \epsilon_{n-1}).$$

Show that T_n is a $2^n \times 2^n$ matrix. Show that its trace is bounded by a number independent of n .

(b) (medium) With the operator norm induced by the function norm, show that \mathcal{T} is a bounded operator.

(c) (hard) Show that \mathcal{T} is not trace class.

15.7. 3-disk fundamental domain cycles. (continued)

from exercise 11.1) Try to sketch $\overline{0}, \overline{1}, \overline{01}, \overline{001}, \overline{011}, \dots$ in the fundamental domain, and interpret the symbols $\{0, 1\}$ by relating them to topologically distinct types of collisions. Compare with table 15.2. Then try to sketch the location of periodic points in the Poincaré section of the billiard flow. The point of this exercise is that while in the configuration space longer cycles look like a hopeless jumble, in the Poincaré section they are clearly and logically ordered. The Poincaré section is always to be preferred to projections of a flow onto the configuration space coordinates, or any other subset of state space coordinates which does not respect the topological organization of the flow.

15.8. 3-disk pruning. (Not easy) Show that for 3-disk game of pinball the pruning of orbits starts at $R : a = 2.04821419\dots$, figure 14.6. (K.T. Hansen)

References

- [15.1] E. Hopf, *Ergodentheorie* (Chelsea Publ. Co., New York 1948).
- [15.2] T. Bedford, M.S. Keane and C. Series, eds., *Ergodic Theory, Symbolic Dynamics and Hyperbolic Spaces* (Oxford Univ. Press, Oxford, 1991).
- [15.3] M.S. Keane, *Ergodic theory and subshifts of finite type*, in ref. [2].
- [15.4] B. Kitchens, "Symbolic dynamics, group automorphisms and Markov partition," in *Real and Complex Dynamical Systems*, B. Branner and P. Hjorth, ed. (Kluwer, Dordrecht, 1995).
- [15.5] R. Bowen, "Markov partitions for Axiom A diffeomorphisms," *Amer. J. Math.* **92**, 725 (1970).
- [15.6] R. Bowen, *Periodic orbits for hyperbolic flows*, *Amer. J. Math.* **94**, 1-30 (1972).
- [15.7] R. Bowen, *Symbolic dynamics for hyperbolic flows*, *Amer. J. Math.* **95**, 429-460 (1973).
- [15.8] R. Bowen and O.E. Lanford, "Zeta functions of restrictions," pp. 43-49 in *Proceeding of the Global Analysis* (A.M.S., Providence 1968).

- [15.9] V.M. Alekseev and M.V. Jakobson, “Symbolic dynamics and hyperbolic dynamical systems,” *Phys. Reports* **75**, 287 (1981).
- [15.10] A. Manning, “Axiom A diffeomorphisms have rational zeta function,” *Bull. London Math. Soc.* **3**, 215 (1971).
- [15.11] W. Thurston, “On the geometry and dynamics of diffeomorphisms of surfaces,” *Bull. Amer. Math. Soc.* **19**, 417 (1988).
- [15.12] P. Cvitanović, G.H. Gunaratne and I. Procaccia, *Phys. Rev. A* **38**, 1503 (1988).
- [15.13] G. D’Alessandro, P. Grassberger, S. Isola and A. Politi, “On the topology of the Hénon Map,” *J. Phys. A* **23**, 5285 (1990).
- [15.14] F. Giovannini and A. Politi, “Generating partitions in Hénon-type maps,” *Phys. Lett. A* **161**, 333 (1992);
- [15.15] G. D’Alessandro, S. Isola and A. Politi, “Geometric properties of the pruning front,” *Prog. Theor. Phys.* **86**, 1149 (1991).
- [15.16] A. de Carvalho, “Pruning fronts and the formation of horseshoes,” *Ergod. Theor. Dynam. Syst.* **19**, 851 (1999).
- [15.17] A. de Carvalho and T. Hall, “How to prune a horseshoe,” *Nonlinearity* **15**, R19 (2002).
- [15.18] Y. Ishii, “Towards a kneading theory for Lozi mappings. I. A solution of the pruning front conjecture and the first tangency problem,” *Nonlinearity* **10**, 731 (1997).
- [15.19] Y. Ishii, “Towards a kneading theory for Lozi Mappings. II: Monotonicity of the topological entropy and Hausdorff dimension of attractors,” *Comm. Math. Phys.* **190**, 375-394 (1997).
- [15.20] S.E. Newhouse, *Topology* **13**, 9 (1974).
- [15.21] S.E. Newhouse, *Publ. Math. IHES* **50**, 101 (1979).
- [15.22] K.T. Hansen, *Symbolic Dynamics in Chaotic Systems*, Ph.D. thesis (Univ. of Oslo, 1994);
ChaosBook.org/projects/KTHansen/thesis.
- [15.23] K.T. Hansen, *CHAOS* **2**, 71 (1992).
- [15.24] K.T. Hansen, *Nonlinearity* **5**.
- [15.25] K.T. Hansen, *Nonlinearity* **5**.
- [15.26] P. Cvitanović and K.T. Hansen, “Symbolic dynamics and Markov partitions for the stadium billiard,” *J. Stat. Phys.*, (accepted 1996, revised version still not resubmitted); [arXiv:chao-dyn/9502005](https://arxiv.org/abs/chao-dyn/9502005).

- [15.27] K.T. Hansen, *Symbolic dynamics IV; a unique partition of maps of Hénon type*, in preparation.
- [15.28] Fa-Geng Xie and Bai-Lin Hao, “Counting the number of periods in one-dimensional maps with multiple critical points,” *Physica A* **202**, 237 (1994).
- [15.29] V. Franceschini and L. Russo, *J. Stat. Phys.* **25**, 757 (1981).
- [15.30] G. D’Alessandro and A. Politi, “Hierarchical approach to complexity ...,” *Phys. Rev. Lett.* **64**, 1609 (1990).
- [15.31] F. Christiansen and A. Politi, “A generating partition for the standard map,” *Phys. Rev. E* **51**, 3811 (1995); [arXiv:chao-dyn/9411005](https://arxiv.org/abs/chao-dyn/9411005).
- [15.32] F. Christiansen and A. Politi, “Symbolic encoding in symplectic maps,” *Nonlinearity* **9**, 1623 (1996).
- [15.33] F. Christiansen and A. Politi, “Guidelines for the construction of a generating partition in the standard map,” *Physica D* **109**, 32 (1997).
- [15.34] C. Simo, “On the analytical and numerical approximation of invariant manifolds,” in D. Baenest and C. Froeschlé, *Les Méthodes Modernes de la Mécanique Céleste* (Goutelas 1989), p. 285.
- [15.35] C. Simo, in *Dynamics and Mission Design Near Libration Points*, Vol. 1-4, (World Sci. Pub., Monograph Ser. Math., 2000-2001).
- [15.36] Y. Lan and P. Cvitanović, “Unstable recurrent patterns in Kuramoto-Sivashinsky dynamics,” *Phys. Rev. E* **78**, 026208 (2004); [arXiv:0804.2474](https://arxiv.org/abs/0804.2474).
- [15.37] T. Hall, “Fat one-dimensional representatives of pseudo-Anosov isotopy classes with minimal periodic orbit structure,” *Nonlinearity* **7**, 367 (1994).
- [15.38] P. Cvitanović and K.T. Hansen, “Symbolic dynamics of the wedge billiard,” Niels Bohr Inst. preprint, unpublished (Nov. 1992)
- [15.39] P. Cvitanović and K.T. Hansen, “Bifurcation structures in maps of Hénon type,” *Nonlinearity* **11**, 1233 (1998).
- [15.40] R.W. Easton, “Trellises formed by stable and unstable manifolds in plane,” *Trans. Amer. Math. Soc.* **294**, 2 (1986).
- [15.41] V. Rom-Kedar, “Transport rates of a class of two-dimensional maps and flows,” *Physica D* **43**, 229 (1990).
- [15.42] V. Daniels, M. Vallières and J-M. Yuan, “Chaotic scattering on a double well: Periodic orbits, symbolic dynamics, and scaling,” *Chaos* **3**, 475 (1993).
- [15.43] P.H. Richter, H.-J. Scholz and A. Wittek, “A Breathing Chaos,” *Nonlinearity* **1**, 45 (1990).
- [15.44] F. Hofbauer, “Periodic points for piecewise monotone transformations,” *Ergod. The. and Dynam. Sys.* **5**, 237 (1985).

- [15.45] F. Hofbauer, “Piecewise invertible dynamical systems,” *Prob. Th. Rel. Fields* **72**, 359 (1986).
- [15.46] K.T. Hansen, “Pruning of orbits in 4-disk and hyperbola billiards,” *CHAOS* **2**, 71 (1992).
- [15.47] G. Troll, “A devil’s staircase into chaotic scattering,” *Pysica D* **50**, 276 (1991)
- [15.48] P. Grassberger, “Toward a quantitative theory of self-generated complexity,” *Int. J. Theor. Phys* **25**, 907 (1986).
- [15.49] D.L. Rod, *J. Diff. Equ.* **14**, 129 (1973).
- [15.50] R.C. Churchill, G. Pecelli and D.L. Rod, *J. Diff. Equ.* **17**, 329 (1975).
- [15.51] R.C. Churchill, G. Pecelli and D.L. Rod, in G. Casati and J. Ford, eds., *Como Conf. Proc. on Stochastic Behavior in Classical and Quantum Hamiltonian Systems* (Springer, Berlin 1976).
- [15.52] R. Mainieri, Ph.D. thesis, New York Univ. (1990); *Phys. Rev. A* **45**, 3580 (1992)
- [15.53] M.J. Giannoni and D. Ullmo, “Coding chaotic billiards: I. Non-compact billiards on a negative curvature manifold,” *Physica D* **41**, 371 (1990).
- [15.54] D. Ullmo and M.J. Giannoni, “Coding chaotic billiards: II. Compact billiards defined on the pseudosphere,” *Physica D* **84**, 329 (1995).
- [15.55] H. Solari, M. Natiello and G.B. Mindlin, “Nonlinear Physics and its Mathematical Tools,” (IOP Publishing Ltd., Bristol, 1996).
- [15.56] R. Gilmore, “Topological analysis of chaotic time series data,” *Revs. Mod. Phys.* **70**, 1455 (1998).
- [15.57] E. Hille, *Analytic function theory II*, (Ginn and Co., Boston 1962).
- [15.58] A. Back, J. Guckenheimer, M. R. Myers, F. J. Wicklin and P. A. Worfolk, “DsTool: Computer assisted exploration of dynamical systems,” *Notices of the AMS* **39**, 303 (1992).
- [15.59] B. Krauskopf and H. M. Osinga, “Investigating torus bifurcations in the forced Van der Pol oscillator,” pp. 199–208 in E. Doedel and L. Tuckerman, eds., *Numerical Methods for Bifurcation Problems and Large-Scale Dynamical Systems, The IMA Volumes in Mathematics and its Applications* **119** (Springer-Verlag, New York 2000).
- [15.60] J. P. England, B. Krauskopf and H. M. Osinga, “Computing one-dimensional stable and unstable sets of planar maps without the inverse,” *J. Applied Dynam. Systems* **3**, 161 (2004).
- [15.61] J. F. Gibson, J. Halcrow, and P. Cvitanović, “Visualizing the geometry of state-space in plane Couette flow,” *J. Fluid Mech.* **611**, 107 (2008); [arXiv:0705.3957](https://arxiv.org/abs/0705.3957).

- [15.62] F. Christiansen, P. Cvitanović and V. Putkaradze, “Hopf’s last hope: spatiotemporal chaos in terms of unstable recurrent patterns,” *Nonlinearity* **10**, 55 (1997); [arXiv:chao-dyn/9606016](https://arxiv.org/abs/chao-dyn/9606016).
- [15.63] S.E. Newhouse, *Topology* **13**, 9 (1974).
- [15.64] S.E. Newhouse, *Publ. Math. IHES* **50**, 101 (1979).
- [15.65] E. Demidov, “Chaotic maps,” www.ibiblio.org/e-notes